Title: Rapid and scale-independent microfluidic manufacture of liposomes entrapping protein incorporating in-line purification and at-line size monitoring.

Authors: Neil Forbes[1+], Maryam T. Hussain[1+], Maria L. Briuglia[2], Darren Y Edwards[3], Joop H. ter Horst[2], Nicolas Szita[4] and Yvonne Perrie [1*]

[1]Strathclyde Institute of Pharmacy and Biomedical Sciences, University of Strathclyde, Glasgow, United Kingdom.

[2]EPSRC Centre for Innovative Manufacturing in Continuous Manufacturing and Crystallisation, University of Strathclyde, Glasgow, United Kingdom.

[3]University of Dundee, Nethergate, Dundee, Scotland, UK, DD1 4HN

[4]Department of Biochemical Engineering, University College London, London, WC1H 0AH, United Kingdom.

[+]these authors contributed equally to this work.

Key Words: Liposomes, protein, microfluidics, manufacture, continuous, scale-independent, formulation.

Corresponding author:

Professor Yvonne Perrie
Strathclyde Institute of Pharmacy and Biomedical Sciences,
161 Cathedral St,
University of Strathclyde,
Glasgow, G4 0RE
Scotland.
yvonne.perrie@strath.ac.uk

Abstract

Within this paper we present work that has the ability to de-risk the translation of liposomes from bench to the clinic. We have used microfluidics for the rapid and scale-independent manufacture of liposomes and have incorporated in-line purification and at-line monitoring of particle size. Using this process, we have manufactured a range of neutral and anionic liposomes incorporating protein. Factors investigated include the microfluidics operating parameters (flow rate ratio (FRR) and total flow rate (TFR)) and the liposome formulation. From these studies, we demonstrate that FRR is a key factor influencing liposome size, protein loading and release profiles. The liposome formulations produced by microfluidics offer high protein loading (20-35 %) compared to production by sonication or extrusion (< 5%). This high loading achieved by microfluidics results from the manufacturing process and is independent of lipid selection and concentration across the range tested. Using in-line purification and at-line size monitoring, we outline the normal operating range for effective production of size controlled (60 to 100 nm), homogenous (PDI <0.2) high load liposomes. This easy microfluidic process provides a translational manufacturing pathway for liposomes in a wide-range of applications.

1. Introduction

Protein-based therapies are a key tool in healthcare with approximately 240 FDA approved protein and peptides available (Fosgerau and Hoffmann, 2015; Lu et al., 2014; Usmani et al., 2017). These proteins and peptides can be used for the treatment and amelioration of a range of diseases as well as used for diagnostic purposes and vaccines (Carter, 2011). However, there are still a number of associated challenges with the delivery of proteins including their sensitivity to both chemical and physical degradation which can result in low bioavailability and short half-life after in vivo administration (Lee and Yuk, 2007). To address this, a wide range of drug delivery systems have been investigated including liposomes. Liposomes can offer targeting, protection to their payload, high biocompatibility and low toxicity (Torchilin and Lukyanov, 2003) and there are a notable number of liposomal formulations on the market or undergoing trials, including a range of anticancer agents, antifungal systems and vaccines such as Inflexal V – a virosome-based vaccine formulation for influenza (Bulbake et al., 2017).

However, the manufacture and production of liposomes is challenging, particularly when considering the entrapment of proteins. Manufacturing conditions including temperature, high pressure, non-aqueous solvents, metal ions, detergents, incompatible pH and/or ionic strength, and shearing can all impact on the chemical and physical stability of proteins. Furthermore, many of the methods adopted give poor encapsulation efficiency, as summarised in Table 1. Although methods such as reverse phase evaporation have been developed to combat some of these issues, this process offers limited size control and produces formulations that are very heterogeneous (Szoka and Papahadjopoulos, 1978). In addition to this, the liposome formulation can also influence protein encapsulation with factors such as the lipid(s) used, the amount of cholesterol and protein concentration all shown to effect the amount of protein encapsulation (Xu et al., 2012).

Microfluidics is an alternative technology that can be used to produce liposomes. It uses a lab-on-a-chip approach and can be defined as the manipulation of small volumes in a controlled microchannel environment, which encourages mixing (Whitesides, 2006). Microfluidics, unlike the thin film lipid hydration method, produces liposomes using a ‘bottom-up’ approach (Akbarzadeh et al., 2013). In contrast to ‘top-down’ methods which rely on size reduction of larger multilamellar vesicles, microfluidics results in the formation of small liposomes from individual lipid monomers and thus no additional size reduction method is needed. Microfluidics offers both ease of scale-up and use for high throughput screening as it can also run with small quantities, whilst maintaining high resolution and sensitivity. This, along with the fact it can decrease production cost and time has led to microfluidics becoming increasingly popular in the pharmaceutical industry.

In microfluidics cartridges, fluid flows through micro-channels that converge; the organic phase (lipids dissolved in alcohol) flows through one channel whilst the aqueous phase (buffer) flows through the other. From the point the two fluid streams converge formation of liposomes begins to occur at the liquid interface. The mixing of the organic phase with the aqueous phase causes a decrease in the concentration of alcohol, due to diffusion (Capretto et al., 2013). As such, the low concentration of alcohol causes an increase in polarity and the lipids to precipitate, resulting in the self-assembly of vesicles with a lipid bilayer and an aqueous core (Jahn et al., 2010; Zook and Vreeland, 2010). Assembly can be controlled by varying the speed (known as the Total Flow Rate (TFR)) and mixing ratio (referred to as the Flow Rate Ratio) of the fluid flows through the channels (Jahn et al., 2007). Recently, several studies have shown the potential of microfluidics to produce liposomes in a range of sizes, as well as encapsulate different materials including small interfering RNA (Belliveau et al., 2012; Chen et al., 2012), low solubility drugs (Kastner et al., 2015), and combinations of aqueous and bilayer drug loaded liposomes (Joshi et al., 2016). Furthermore, Dimov et al (Dimov et al., 2017), demonstrated a lab-on-bench scale set-up for the manufacture of liposomes in a scale independent manner using novel engineered equipment. Nonetheless, whilst research has shown the ability to encapsulate a range of biologics, the ability to scale up this process has not been systematically explored. Therefore, within this paper we investigate and demonstrate the use of microfluidics to encapsulate proteins in a scale-independent manner and we incorporate in-line purification and at-line particle size monitoring for in-process control and as a product validation tool.

2. Materials and Methods.

2.1 Materials

The lipids egg phosphatidylcholine (PC), 1,2-dimyristoyl-sn-glycero-3-phosphocholine (DMPC), 1,2-dipalmitoyl-sn-glycero-3-phosphocholine (DPPC), 1,2-distearoyl-sn-glycero-3-phosphocholine (DSPC), and L-α-phosphatidylserine (Brain PS, Porcine) were all purchased from Avanti Polar Lipids Inc., Alabaster, AL, US. Cholesterol (cholesterol), Insulin, Ovalbumin (OVA), bovine serum albumin (BSA), Sucrose, trifluoroacetic acid and D9777-100ft dialysis tubing cellulose were purchased from Sigma Aldrich Company Ltd., Poole, UK. For ovalbumin purification by Tangential flow filtration (TFF), a modified polyethersulfone (mPES) 750 kD MWCO hollow fibre column was used (Spectrum Inc., Breda, The Netherlands). For release studies, Biotech CE Tubing MWCO 300 kD was used (Spectrum Inc., Breda, The Netherlands). A Jupiter column (C18 (300 Å), 5 µm, dimensions 4.60 X 150 mm) and a Luna column (C18(2), 5 µm, dimensions 4.60 X 150 mm, pore size 100 Å) was used in HPLC and purchased from Phenomenex., Macclesfield, UK. The Pierce™ BCA Protein Assay kit, Dil Stain (1,1'-Dioctadecyl-3,3,3',3'- Tetramethylindocarbocyanine Perchlorate ('Dil'; DilC18 (3)), HPLC grade methanol and 2-

propanol were purchased from Fisher Scientific, Loughborough, England, UK. All water and solvents used were HPLC grade.

2.2. Liposome production

2.2.1 Liposomes prepared by extrusion and sonication

Lipids were dissolved at required concentrations in a chloroform:methanol mixture (v/v 9:1) and placed under vacuum via rotatory evaporation for 6 minutes at 200 rpm in a heated (37°C) water bath to remove solvent. Hydration of the lipid film and protein encapsulation was achieved by the addition of phosphate buffered saline (PBS) (pH 7.3 ± 0.2) containing ovalbumin (0.25 mg/mL) at temperatures above the appropriate lipid transition temperature. Hand held extrusion was conducted on multilamellar vesicles (MLV) using a Mini Extruder from Avanti Polar Lipids Inc., Alabaster, AL, US. Liposomes (1 mg/mL) were extruded through incrementally decreasing pore sized membranes (0.5 – 0.2 µm), with each sample being cycled through ten times. During extrusion, liposomes were held above their appropriate transition temperature. Size reduction of multilamellar vesicles was also achieved via sonication using a 9.5 mm titanium probe sonicator (Soniprep 150, MSE labs, UK) for 4 minutes at 10 Hz. Again during this process, liposomes were held above their appropriate transition temperature.

2.2.2. Liposomes prepared by microfluidics

The preparation of liposomes by microfluidics was conducted on the Nanoasemblr® Benchtop system from Precision Nanosystems. Selected lipids were dissolved in methanol at specific concentrations (ranging primarily between 0.3 – 10 mg/mL total lipid) and injected through one of the two inlets on the microfluidics herringbone micromixer chip, whilst the aqueous phase (PBS; pH 7.3 ± 0.2) is injected into the second inlet. A number of production parameters can be controlled using the Nanoassemblr® software including the flow rate ratio (the ratio between the aqueous phase and the lipid phase) and the total flow rate (the speed at which the two inlets are injected through the chip). Flow rate ratios of 1:1, 3:1 and 5:1 were selected for testing as well as total flow rate speeds between 5 - 20 mL/min. For the production of protein loaded liposomes, ovalbumin was added to the aqueous phase at specific concentrations and the same principles for the production of empty liposomes was followed. Larger scale production of OVA loaded liposomes was prepared using the Nanoassemblr® Blaze™ (10 mL to 1L) utilising the same production parameters as previously optimised on the Benchtop system (3:1 FRR, 15 mL/min), without the addition of a dilution factor.

2.3. Quantification of lipid and liposome recovery

HPLC- ELSD (high performance liquid chromatography- evaporative light scattering detector) was used to quantify the lipid recovery within liposomes. A Luna column (C18(2), 5 µm, dimensions 4.60 X 150 mm, pore size 100 Å) was used to detect the lipids, at a flow rate of 2 mL/min. A twenty minute elution gradient, composed of solvent A (0.1% TFA in water) and solvent B (100% methanol) was used. During the first six minutes the gradient was 15:85 (A:B), at 6.1 minutes 0:100 (A:B) and then back to the initial gradient of 15:85 (A:B) from 15.1 to 20 minutes. The lipid recovery was calculated as a percentage in comparison to the initial concentration of the stock solution. Liposome recovery was calculated by incorporating the hydrophobic dye DiI Stain (1,1'-Dioctadecyl-3,3,3',3'-Tetramethylindocarbocyanine Perchlorate ('DiI'; DilC18 (3)) (DilC) at 0.2 mol% into the bilayer of the liposomes. Post production and during purification, aliquots of permeate was collected during the TFF process.

2.4 Liposome purification via tangential flow filtration

Liposome samples were purified using Krosflo Research Iii tangential flow filtration system fitted with an mPES (modified polyethersulfone) column with a pore size of 750 kD. For removal of solvent and unentrapped protein, liposomal samples were circulated through the column and purified through difiltration, with fresh PBS being added at the same rate as the permeate leaving the column.

2.5. Liposome characterisation

Dynamic light scattering (DLS) was used to analyse the intensity mean diameter (z-average) and polydispersity index (PDI) of the liposomal formulations using a Malvern Zetasizer Nano-ZS (Malvern Instruments, Worcs., UK). All measurements were undertaken in triplicate. All readings were between 6-9 attenuation and samples were diluted 1/10 with appropriate buffer. To continuously monitor particle size in an at-line process, the Zetasizer AT (Malvern Panlaytical Ltd, Malvern, UK) was used. The Zetasizer AT measured liposome size and PDI at a 1:10 dilution (liposomes to buffer). A buffer flow rate of 5 mL/min and liposome formulation flow rate of 0.5 mL/min were used. A total of 1 mL was required for each size measurement.

2.6. Liposome morphology

Images were taken on a Jeol 2011 with a 200kv beam using minimal dose protocol, scanned at low magnification and jumped to high magnification without exposing the sample to the beam first. The camera used was a Gatan ultrascan (2k by 2k pixels). Grids were lacey carbon, 200 mesh and were prepared by adding 8 microlitres of sample to a glow discharged grid, blotting from both sides for

approximately 5 seconds then plunging into nitrogen cooled ethane propane mix (70% ethane). CryoTEM pictures were taken at Warwick University, UK by Dr Saskia Bakker, Advanced Bioimaging Platform, and University of Warwick. Evaluation was performed at 15000x magnification.

2.7. Encapsulated protein quantification

Solubilisation of the liposomes to release entrapped protein was achieved following a previously published protocol (Fatouros and Antimisiaris, 2002) and modified for protein formulations. Briefly, liposomal samples were added at a 50/50 v/v ratio with solubilisation mixture (PBS / 2-Propanol 50/50 v/v) and vortexed. Protein quantification was then determined using either UV-HPLC or BCA protein assay. For UV-HPLC, an Agilent 1100 Series HPLC (California, USA) was used to quantify the amount of OVA entrapped inside liposomes. All samples were run at 280 nm, using a C18 column (i.d. 150 X 4.6 mm) from Phenomenex (Macclesfield, UK). A 1 mL/min flow rate was used with a twenty minute elution gradient, composed of solvent A (0.1% TFA in water) and solvent B (100% methanol). During the first ten minutes the gradient was 100: 0 (A: B), at 10.1 minutes 0: 100 (A: B) and then back to the initial gradient of 100: 0 (A: B) from 15.1 to 20 minutes. The injection volume for the sample is 20 µL. For protein release studies, HPLC was used in conjunction with a SEDEX 90LT evaporative light scattering detector (ELSD) (Sedex sedere, Alfortville, France) to quantify the amount of OVA. A Jupiter A100 column was used to detect the OVA protein. The flow rate used was 1 mL/ min, with a gain of 8 and an OVA peak appearing at 11.8 minutes. A standard calibration curve for OVA was established using various concentrations; the amount of encapsulated protein in liposomes produced by microfluidics and sonication was calculated using the peak area of the sample in relation to the standards. Protein quantification using BCA/ Micro BCA protein assay was carried out as per manufacturer's instructions. Briefly, samples were incubated with appropriate volume of working reagent and incubated at 37°C and the absorbance measured at 562 nm. Calibration curves were subjected to the inclusion of empty liposomes and solubilisation mixture and appropriate blanks were measured for subtraction of absorbance values.

2.8 Circular dichroism

The OVA protein integrity was tested after microfluidics and TFF. Untreated OVA (0.3 mg/ mL) in PBS was used as a control to test OVA integrity inside DSPC:Chol liposomes. The liposomes were made using 8 mg/mL initial lipid and 8 mg/ mL initial OVA at a 3:1 FRR and 15 mL/min TFR. The Chiroscan™-plus was used to analyse OVA using 20 µL of the respective samples. The sample was placed in between two microscope slides and placed into a Suprasil® quartz absorption cuvette (Hellma,

Germany: path length of 1 mm). The measurement temperature was 25 °C and spectra recorded from 180-260 nm range.

2.9 Protein release studies

Ovalbumin loaded liposomes (PC:Chol, DMPC:Chol, DPPC:Chol and DSPC:Chol) were produced using microfluidics using a 3:1 FRR and 15 mL/min TFR (4 mg/mL initial lipid and 0.25 mg/mL Ovalbumin). The DMPC:Chol formulation was selected, and made at both a 3:1 and 5:1 FRR (the TFR used was 15 mL/min). The unentrapped OVA and solvent was removed by TFF (12 mL wash cycle needed per mL of formulation). Purified formulations are used to investigate the rate of OVA release; 1 mL of the formulation was placed in a 300 kD dialysis bag in the presence of 25 mL of phosphate buffered saline (pH 7.3 ± 0.2). The samples were left for 0.5, 1, 3, 6, 18, 24, 48, 72, 96 and 120 hours at 37°C with agitation, after the allocated time the liposome formulation was collected and analysed by HPLC.

2.10 Headspace Gas Chromatography

Headspace gas chromatography (Agilent 7697A, Agilent Technologies, USA) was used to measure residual solvent content for liposomes produced by microfluidics and purified by tangential flow filtration. Solvent was measured using in an isothermal process using an Agilent 122-1334 column (30m x 250µm x 1.4 µm). The sample was held at 60°C for a minute before the temperature was ramped up to 80°C for 6 minutes.

2.11 Statistical analysis

Results are represented as mean ± SD with n = 3 independent batches. ANOVA tests were used to assess statistical significance, with a Tukey's post adhoc test (p value of less than 0.05). Where appropriate the similarity or differences between drug release profiles from various formulations was assessed by the f_2 similarity test.

3. Results and Discussion

3.1 Rapid and scalable manufacture of liposomes prepared by microfluidics: identifying the normal operating range.

We have previously reported on the use of microfluidics to manufacture liposomes entrapping DNA (Kastner et al., 2015), low soluble drugs (Dimov et al., 2017; Kastner et al., 2015) and combinations of high and low soluble drugs (Joshi et al., 2016). To investigate this manufacturing method for the production of liposomes entrapping proteins, we first set out to identify our working parameters in terms of the effect of lipid selection, initial lipid concentration, flow rate ratio, total flow rate and manufacturing temperature (given the potential sensitivity of drugs and proteins to temperature

instabilities). To achieve this, four liposome formulations were prepared using phospholipids with increasing hydrocarbon tail length (and lipid phase transition temperature) i.e. PC:Chol, DMPC:Chol, DPPC:Chol and DSPC:Chol. Liposomes were produced at a 3:1 FRR and a 15 mL/min TFR and the effect of the hydrocarbon tail length of the PC on the resulting liposomes size and PDI was investigated post solvent removal (Figure 1).

Results in Figure 1A show that as we increase our phospholipid alkyl chain length (from PC up to DSPC) we see a trend of decreasing vesicle size. This trend of decreasing liposome size with increasing alkyl chain length is evident across all concentrations tested (from 0.3 mg/mL to 10 mg/mL; Figure 1A). For example, at the lowest lipid concentration tested (0.3 mg/mL initial concentration) liposomes reduced significantly ($p<0.05$) from approximately 100 nm down to 60 nm in size. At the highest lipid concentration (10 mg/mL), the reduction was less notable but still significant ($p<0.05$) with liposomes reducing from 70 to 45 nm (Figure 1A). Figure 1A also shows that with increasing initial lipid concentrations, liposome size also decreases irrespective of the lipid selected (Figure 1A); as we increase from 0.3 to 10 mg/mL initial lipid concentration, PC liposomes reduce from approximately 100 nm to 70 nm, DMPC liposomes reduce from 75 to 60 nm, DPPC liposomes reduce from 70 to 45 nm, and DSPC liposomes reduce from 55 to 45 nm; Figure 1A). This link between lipid concentration and liposome size is in line with previously reported studies (Joshi et al., 2016) where we investigated PC:Chol liposomes. In Figure 1A we now demonstrate this effect applies to a range of liposome formulations and the lipid recovery after microfluidic production was also high (>94%) for all 4 formulations tested (Table 2).

To consider if the reduction in vesicle size was related to lipid alkyl chain length or lipid transition temperature, we also compared liposomes prepared using two lipids with the same alkyl chain length (18 carbons) but different transition temperatures: DSPC (Tm of 55^{o}C) and DOPC (Tm of -17^{o}C). Table 3 shows that liposomes formed using DOPC were approximately 40 nm larger in size than DSPC. This suggests that whilst adopting longer alkyl chain length PCs within the liposome formulation can reduce vesicle size, the degree of saturation and the ability of these PC to pack within a bilayer must also be considered. Irrespective of the lipid concentration, the lipid transition temperature and lipid alkyl chain length, all liposome formulations were produced with low PDI values (<0.2; Figure 1B) demonstrating the highly homogenous nature of the liposomal products produced via microfluidics. Thus, across all formulations, liposomes could easily be formulated to sizes below 100 nm with low PDI values.

Generally in the production of liposomes using lipid-hydration methods, liposomes must be formed above their transition temperature (Szoka Jr and Papahadjopoulos, 1980) with for example DSPC

liposomes commonly being prepared above 55°C. This can present issues for thermo-liable drugs and proteins. However, the addition of 50% mol/mol cholesterol has been shown by differential scanning calorimetry to abolish the gel-to-liquid phase transition temperature of DSPC liposomes (Moghaddam et al., 2011). To investigate if such increased temperatures are required for liposome production using microfluidics, we prepared various DSPC liposome formulations with increasing cholesterol concentrations (from 10:1 to 10:5 wt/wt ratio equivalent to 5 to 50 mol%; initial lipid concentration of 4 mg/mL) at a range of process temperatures (controlled within the Nanoassemblr™) from room temperature to 60°C (Figure 1C and 1D). The results demonstrate that all liposome formulations could be prepared at room temperature with no impact on the liposome size, irrespective of the transition temperature of the cholesterol concentration or the main PC lipid (in this case 55°C). The key factor controlling the liposomes size across these formulations is the cholesterol content (Figure 1C); increasing cholesterol content reduces liposome size from approximately 150 nm (10:1 wt/wt ratio) down to around 50 nm when equimolar DSPC:Cholesterol is employed as the formulation. Again whilst the formulation composition was shown to impact on the liposome size, there was no impact on the homogenous nature of the liposome suspensions with all formulations showing PDI values below 0.2 (Figure 1D). These results demonstrate liposome formulations with a range of transition temperatures can be prepared using microfluidics without employing heating thereby circumventing any concerns of heat-induced degradation of the drug/lipids being incorporated.

The ability to manufacture liposomes from high transition temperature lipids without the need to work above the phase transition temperature of the lipids is a strong attribute of this manufacturing method as it circumvents risks of thermo-instability issues. The ability to manufacture liposomes at room temperature, irrespective of the transition temperature of the lipids incorporated, may result from the rapid 'bottom up process' of microfluidics. In this process, the liposomes are formed from individual monomers, thus the phase transition of the lipids in the bilayer does not influence the process compared to other methods where lipids need to be hydrated into liposomes and bilayers need to break-down and reform. Whilst the presence of cholesterol in formulations can help with this process by reducing transition temperature of the bilayer, this is generally only at molar concentrations of 50 % (Moghaddam et al., 2011). Cholesterol is commonly incorporated into liposomal formulations due to its well documented ability to enhance the stability of the vesicles and reduce drug leakage and membrane permeability, as first reported by Gregoriadis and Davis, (1979). Cholesterol enhances the stability of liposome bilayers by increasing the packing densities of the phospholipids (Semple et al., 1996) due to the cholesterol packing within molecular cavities formed by the lipid molecules as they arrange in the bilayer (Devaraj et al., 2002). This space-filling action of cholesterol thereby results in a more compact bilayer (Epand et al., 2003). This increased packaging

of the lipids and compact bilayer maybe the driver behind the smaller liposome sizes produced at higher cholesterol concentrations (Figure 1C). As mentioned, the addition of 50% mol/mol cholesterol has been shown by differential scanning calorimetry to abolish the gel-to-liquid phase transition temperature of DSPC liposomes (Moghaddam et al., 2011). However, at all concentrations tested (5 to 50% mol/mol; Figure 1C and D), liposomes can be manufactured without the need to work at temperatures above the transition temperature of the main (DSPC) lipid. This confirms that the bottom-up building of the liposomes from monomers during the microfluidic process negates the need for heating during the production of liposomes irrespective of their lipid transition temperature. The initial solubility of the lipids in solvents may still be a consideration for some formulations and can be improved via adopting increased temperatures. However, across all the formulations and concentrations tested within these studies no heating was required in the processes.

Given that our results demonstrate both the initial lipid concentration and lipid choice impact on the size of liposomes formed, we further investigated the impact of the flow rate ratio at which we mix our solvent and aqueous phases during liposome production. Figure 2A to C demonstrate the effect of initial lipid concentration and flow rate ratio on the size and PDI of liposomes formed from DSPC:Chol (10:5 wt/wt). As can be seen, a flow rate ratio of 1:1 can be used to form larger liposomes (100 to 200 nm depending on the initial lipid concentration selected; Figure 2A) compared to the 3:1 and 5:1 mixing flow rate (Figure 2B and C respectively). These larger liposomes formed at the 1:1 flow rate are not linked to an increasingly heterogeneous liposomes population as in all cases the PDI remains low (≤0.2; Figure 2A). By increasing the flow rate ratio to 3:1, we can produce liposomes in a smaller size range (50 to 60 nm) again with a low PDI (≤0.2) (Figure 2B). When working at 5:1 flow ratios, we tend to see more heterogeneous populations with slightly higher PDI values unless higher initial lipid concentrations are used (above 2 mg/mL; Figure 2C). Given these results, we also considered the normal operating range for anionic liposomes (DSPC:Chol:PS; 10:5:4 wt/wt) (Figure 2D). From these results we see that at a 3:1 flow ratio, liposomes of 50 to 60 nm are produced across the range of concentrations tested with initial lipid concentrations of 2 mg/mL and above giving us PDI values of <0.2 (Figure 2D). We further considered the rate at which we could produce our liposomes by considering flow rates of 5 to 20 mL/min. Figure 2E and 2F confirms we can produce liposomes within the same size range and low PDI at a range of flow rates with no significant difference between the batches produced. These results demonstrate we can apply similar operating parameters for both neutral and anionic formulations and achieve highly reproducible and homogenous liposome formulations.

Previous studies by Kastner et al using liposomal formulation DOPE:DOTAP and PC:Chol on a staggered herringbone micromixer chip show a reduction in average liposome size as the flow rate ratio was

increased from 1:1 to 5:1. The average liposome size of the formulations at a flow rate ratio of 1:1 resulted in sizes above 200 nm, while a flow rate ratio of 5:1 generated sizes around 50 nm (Kastner et al., 2014) (Kastner et al., 2015). Similar results were obtained by Jahn et al where the authors showed that as the flow rate ratio was increased, the resulting particle size decreased. This was attributed to the difference in the alcohol content of the flow rate ratios, as the flow rate ratio decreases the amount of alcohol injected into the stream increases. When the lipids in alcohol first come in contact with the aqueous stream, liposomes will self-assemble and form at the interface. As the streams then continue to mix, the initially formed liposomes take alcohol up and reach the critical alcohol concentration resulting in some partial disassembly, the continuing mixing will then decrease the alcohol concentration in the liposomes again, resulting in re-assembly. When the flow rate ratio is increased, the overall alcohol concentration is reduced, thus the amount of liposomes exposed to fluctuating increases and decreases of alcohol is reduced thus limiting the assembly / re-assembly cycle (Jahn et al., 2010) (Jahn et al., 2007). Similar findings were also reported by Zizzari et al for the liposomal formulation HSPC:Chol:mPEG-2000-DSPE produced over a range of flow rate ratios. Again, Zizzari et al note that at higher flow rate ratios, a smaller solvent stream results and as the lipid discs form at the liquid interface they begin to bend, eventually forming a vesicular particle as a result of surface area of the hydrophobic chains in the presence of decreasing solvent concentration. The length of time these lipid discs are allowed to grow will directly impact upon the final vesicle size, with shorter times leading to smaller liposomes. Thus at lower flow rate ratios (e.g. 1:1), the higher the concentration of solvent and thus the longer the time the lipid discs have to expand (Zizzari et al., 2017). Whilst the flow rate ratio has been shown to impact upon liposome size and thus should be tested to identify the normal operating range for a given formulation, the total flow rate (TFR mL/min) did not impact on the liposome size and with the formulations tested a flow rate of 5 to 20 mL/min is a proven acceptable range to work within. This is in line with previous work reported by Joshi et al where again the flow ratio was shown to impact on particle size of PC:Chol liposomes, but flow rate had no impact across all speeds tested (Joshi et al., 2016). Therefore, we have established that by choosing the appropriate initial lipid concentration in the tested range of flow rates, we can control liposome size and maintain low (<0.2) PDI values through selection of flow ratios in combination with the initial lipid concentration. For all formulations, a heating step can be eliminated circumventing any potential thermal protein denaturation occurring.

3.2 Purification and concentration of liposomal systems.

To ensure removal of residual solvent and non-incorporated protein, liposomes were purified via tangential flow filtration (TFF). To validate the purification process and confirm solvent removal, residual solvent levels were quantified via headspace gas chromatography (Figure 3A). Results show

that after 12 wash cycles solvent levels were below ICH guidelines of less than 3000 parts per million (or less than 0.3% of residual solvent remaining) (International conference in Harmonisation, 2016 (ICH)). Similarly, this wash cycle was able to remove all non-incorporated protein (Figure 3B). This was confirmed by mixing pre-prepared 'empty' liposomes and with various protein concentrations. Given the protein was not entrapped, 100% removal confirms all free protein can be removed. Figure 3C, confirms the TFF process has no detrimental effect on the liposome attributes with the particle size, PDI and morphology remaining unchanged, and liposome recovery was high (95-100%; results not shown).

Using TFF, we were also able to concentrate both the neutral (Figure 4A and B) and anionic liposome formulations (Figure 4C and D) up to 4 fold, without any determent to their vesicle attributes with four cycles being sufficient to double the concentration of liposomes. The recovery of the liposomes was again 95-100% (results not shown) similar to studies where a lab-on-chip TFF purification system was adopted (Dimov et al., 2017). The ability to purify liposome formulations in a scalable format is an important feature of any manufacturing process. Furthermore, the lipid solubility of some lipids within suitable solvents can be limited and thus TFF can allow the concentration of liposome formulations to required doses. These studies demonstrate the ability to purify and/or concentrate liposome formulations in scalable format.

3.3 Scale-independent manufacturing of liposomes entrapping proteins.

Now that we have identified the normal operating range for the microfluidic production and appropriate purification protocols for a range liposome formulations, we can next consider protein loading of these liposomes. First, we compared protein loading of liposomes composed of DSPC:Chol (10:5 wt/wt) prepared by microfluidics, sonication and extrusion. Liposomes produced by microfluidics gives high protein loading (25 – 35%; 250 μg/mL initial protein concentration), whilst both sonication and extrusion gave low (< 5%) protein loading (Figure 5A). Microfluidics also produced small vesicles (60 to 70 nm; PDI 0.2) similar in size to 'empty' liposomes and notably smaller and more homogeneous than vesicles formed from sonication or extrusion (Figure 5A). The similarity in size between loaded and unloaded liposomes suggests that in the initial process development, empty liposomes can be used, reducing the amount (and cost) of active pharmaceutical ingredient used.

The effect of extrusion on protein loaded MLVs has previously been shown to reduce the concentration of protein entrapped within the vesicles following extrusion cycles. Large particles that cannot flow through are blocked at the membrane pores and the pressure from the extrusion process ruptures the liposomes (Patty and Frisken, 2003). This rupturing coincides with a major decrease in the encapsulation efficiency of the protein after the first extrusion cycle and the retention of the

protein upon the filter (Colletier et al., 2002). This presents protein entrapment issues if progressively smaller and smaller membrane filters are used during the extrusion process to downsize MLVs to size ranges below 100 nm (which are easily achieved via microfluidics). Similarly, probe sonication of liposome formulations for size reduction leads to poor encapsulation efficiencies, generally below 10 % for aqueous soluble macromolecules (Lapinski et al., 2007). Although sonication is widely used to break down MLVs by acoustic energy (Mendez and Banerjee, 2017), there is little control of the end product with batch to batch variation. A lack of temperature control can also present challenges for protein encapsulation, and depending on the system, the need to remove contamination post sonication is an added step to production (Philippot and Schuber, 2017). In comparison, the rapid production processes, coupled with higher encapsulation efficiencies of protein, demonstrates that microfluidics is an effective method for one step, scalable production of protein loaded liposomes.

When produced via microfluidics, the choice of lipid used within the liposome formulation has no significant impact on protein loading with liposomes composed of PC, DMPC, DPPC and DSPC all showing similarly high (30-40%) protein loading (Figure 5B). These formulations were prepared at room temperature and Figure 5C shows that the ovalbumin (OVA) contained in liposomes and the untreated OVA have a similar CD spectra. In addition, the CD spectrum, containing information on the OVA structure, with nine alpha helical structures and two beta sheets (Stein et al., 1990), is in keeping with literature (Paolinelli et al., 1997). Therefore, it is concluded from the CD measurements that the entrapped protein retained its structural conformation during liposome production.

We again investigated the influence of lipid concentration on these systems, this time in relation to protein encapsulation. Varying amounts of PC, DMPC, DPPC and DSPC liposomes (from 0.5 to 10 mg/mL initial lipid concentration) were used and the encapsulation efficiency of OVA (250 µg/mL) tested. This was plotted on a double logarithmic plot of the encapsulation versus lipid concentration as previously done by Colletier et al. (Colletier et al., 2002) (Figure 5D). The authors suggest to do this as the total liposome surface area is proportional to the lipid concentration, yet the encapsulated inner volume is proportional to the lipid concentration to the power 3/2. Thus the double log plot allows the discrimination between the relevant parameters (Colletier et al., 2002). With all 4 liposome formulations, the data shows a relatively good linear correlation (R^2 >0.9). It has been proposed that if the gradient is close to 1 then encapsulation is proportional to the number of lipids and the surface area, and if the slope is close to 1.5 this suggest that encapsulation is related to internal volume. Whilst the plot of DMPC:Chol can be seen to have a gradient close to 1, PC, DPPC and DSPC are notable lower than 1 and all 4 are far from 1.5. This suggests that the high incorporation of protein within liposomes using microfluidics is a factor of the manufacturing process and less influenced by the number of lipids or by the internal volume.

We further studied the protein loading efficiency of both neutral (DSPC:Chol; 10:5 wt/wt) and anionic (DSPC:Chol:PS; 10:5:4 wt/wt) liposomes at a fixed lipid concentration and increasing protein concentrations. Figure 6A shows that up to an initial protein concentration of 2 mg/mL protein encapsulation efficiency remains high at approximately 30 %, which is equivalent to approximately 400 µg/mL prior to any concentration steps. Over this protein concentration range, the liposome size and PDI remained stable at around 60 – 80 nm and PDI of ~0.2 (Figure 6B), with a near neutral zeta potential (Figure 6C). Increasing the protein concentration further, to 10 mg/mL, caused a drop in encapsulation efficiency (15%) but an increase in the total amount of OVA loaded. However, it also resulted in aggregation and large particle sizes (above 700 nm; results not shown). Anionic liposomes (Figure 6D – F) also gave good protein loading over the same range (0.1 to 2 mg/mL initial protein concentrations) with entrapment efficiencies of ~ 20 % (Figure 6D) and the protein loading within the liposomes does not influence their particle size, PDI nor zeta potential over this range (Figure 6E and F).

The decrease in entrapment efficiency with the anionic liposomal formulation compared to the neutral formulation is not un-common. Colletier et al also investigated the effect of charge on the entrapment efficiencies of acetylcholinesterase using a neutral lipid POPC and an anionic lipid POPS. Using multiple freeze-thaw cycles, the anionic formulation achieved an encapsulation efficiency around 20% while the neutral POPC formulation achieved around 40% acetylcholinesterase encapsulation indicating the electrostatic interactions between proteins peripheral charge and the polar head group of the phospholipids has a substantial control over the ability of the entrapment process within the vesicles (Colletier et al., 2002).

The effect of flow ratio and flow rate was also considered for both these liposome formulations (Figure 7). Only flow rates of 3:1 and 5:1 were considered as a flow ratio of 1:1 was shown to result in aggregation which may be a result of protein aggregation at high (50%) solvent concentrations (results not shown). Increasing the flow rate from 3:1 to 5:1 was shown to reduce protein loading by approximately 10% and increasing the variability in the particle size of the DSPC:Chol liposomes (Figure 7A and B respectively). Working at flow rate of 10 mL/min or above also gave reproducible protein loading (20 – 25%; 700 µg/mL initial ovalbumin concentration), particle size (55 – 65 nm) and PDI (~0.2) (Figure 7C and D). This is again comparable to our data with empty liposomes (Figure 2). Similar results were shown with the anionic liposomes (DSPC:Chol:PS); increasing the flow rate ratio from 3:1 to 5:1, significantly ($p<0.05$) reduced protein loading from 20% to 9% (Figure 7E) without influencing liposome size (100 – 110 nm; Figure 7F). Again working at a flow rates of 10 mL/min or more giving protein loading of 20 – 25 % with no significant impact on protein loading (Figure 7G) nor particle size (which remained around 100 to 120 nm; Figure 7H). With both formulations, working a low flow rate

of 5 mL/min did reduce protein loading despite particle size remaining the same. This again suggests that protein entrapment efficiency is controlled more by the manufacturing than the lipid/protein concentrations and thus can be easily scaled within identified normal operating ranges.

In order to determine the effect of flow rate ratio on the protein encapsulation efficiency, the final lipid and protein concentrations described in figure 7 were matched by adjusting the initial concentrations. Despite controlling for these variables, a significantly lower protein entrapment efficiency is observed when the flow rate ratio is increased from 3:1 to 5:1. The difference in encapsulation efficiency between the flow rate ratios could be due a shift in position of the liquid-liquid interface between the two different flow rate ratios during liposome production in the chip (Oellers et al., 2017). At a 1:1 FRR the liquid-liquid interface (the mixing of the solvent and aqueous phase) occurs at the centre of the chip, with this position changing in accordance to the FRR selected. Carugo et al also note that changes in the flow rate ratio have a direct impact upon the fluid stream, thus altering the properties of the fluidic environment within the chip which could impact upon the interactions between the lipid phase and aqueous protein during liposomal formation (Carugo et al., 2016).

Given the various parameters for optimal loading have been established, these parameters were then tested with two additional proteins (Table 4) and in a 10 times scaled process (Figure 8). Table 4 demonstrates that both a smaller protein (insulin) and larger protein (bovine serum albumin) can also be effectively entrapped (25 to 37 %) within DSPC:Chol liposomes prepared using the optimised parameters, with liposomes in a similar size range (55 - 70 nm) being produced. Furthermore, to demonstrate the scalability of the process, two batches of liposomes (DSPC:Chol) were prepared by either the small-laboratory scale NanoAssemblr® Benchtop (1 -15 mL batch size) and the larger Blaze™ (10 mL to 1 L batch size) entrapping OVA. Across both platforms, liposomes were manufactured with reproducible results in terms of protein loading and particle attributes (Figure 8), demonstrating the easy scale-up of the process developed.

3.4 Release characteristics of liposomes entrapping protein

The ability of liposome formulations to retain, delivery and release protein is important. Release profiles of protein in-vitro can be used to determine behaviour in vivo. The release rate of protein from liposomes is highly dependent on factors such as liposome composition and the nature of the protein entrapped (Panagi et al., 1998). The effect of liposome composition was investigated using four neutral liposomes containing cholesterol. Lipids with varying carbon chain lengths were tested to investigate the effect of tail length on release. Figure 9A shows all four neutral formulations (PC:Chol, DMPC:Chol, DPPC:Chol and DSPC:Chol) are capable of protein release. The general trend observed

confirms previous research whereby, the longer hydrocarbon tailed lipids used the slower the release (e.g. Panagi et al., 1998). OVA is fully released from PC:Chol liposomes within 72 hours, meanwhile both DPPC:Chol and DSPC:Chol do not fully release OVA by 120 hours; there is 9% OVA remaining for DPPC:Chol and 47% OVA remaining for the DSPC:Chol liposomes after 5 days. The findings are in keeping with previous studies showing liposomes formulated from longer chain lipids have slower release rates due to their increased bilayer rigidity. Longer chain lipids, such as DSPC, have more opportunity to create Van der Waals forces between the longer hydrocarbon tails and improved membrane packing compared to liposomes composed of shorter chain phosphatidylcholines (Mohammed et al., 2004; Panagi et al., 1998). Moreover, the release profiles for PC:Chol, DMPC:Chol and DPPC:Chol liposomes prepared by microfluidics match previous studies whereby a burst release is observed within the first 12 hours, after which a slower rate of release is observed (Monteiro et al., 2014; Murao et al., 2002; Panagi et al., 1998).

In addition, given the ability to manipulate the flow rate ratio to change liposomal formulation characteristics, the effect of this ratio on protein release from liposomes was investigated. Two formulations (DMPC:Chol and DSPC:Chol) were used to investigate any possible changes in release caused by the selected manufacturing process. The encapsulation efficiency for DMPC:Chol liposome formulations produced at a 3:1 FRR is 37 ± 0.2 % and 29 ± 0.6 % for DMPC:Chol liposomes produced at a 5:1 FRR. Figure 9B shows the 5:1 FRR releases the protein OVA at a faster rate in comparison to the DMPC:Chol liposomes produced at a 3:1 FRR with a similarity factor (f_2) of 24.6 being calculated (it is generally accepted that an f_2 of 50-100 suggests similar release profiles). The same pattern is also observed for OVA loaded DSPC:Chol liposomes produced at a 3:1 and 5:1 FRR (Figure 8C), with the DSPC:Chol liposomes produced at a 5:1 showing a faster release rate (f_2 of 48.3) than DSPC:Chol liposomes produced at 3:1 despite the amount of protein loaded within these formulations being matched (0.1875 ug/mL final OVA concentration). Similar to the differences noted in encapsulation efficiency of the liposomes produced by FRRs, a range of factors may be responsible for the effect of flow rate ratio on release rate. As previously mentioned, when the flow rate ratio is increased, the alcohol concentration is reduced, which reduces the opportunity for liposomes to re-assemble during their production (Jahn et al., 2010) (Jahn et al., 2007). Also at lower alcohol concentrations, there is less time for lipid discs to expand and form liposomes (Zizzari et al., 2017); different flow rate ratios result in a shift in position of the liquid-liquid interface (Oellers et al., 2017). Each or all of these factor may impact on the assembly of the liposomal bilayers which in turn will impact on release profiles. A shift in the position of the liquid-liquid interface and/or differences in the ethanol concentrations could result in subtle changes in the cholesterol tilt within the liposome bilayers. Indeed, the position of cholesterol is highly variable with concentration and production method used. Research by

Khelashvili and Harries (Khelashvili and Harries, 2013; Khelashvili et al., 2010), has shown that DMPC:Chol liposomes with a cholesterol concentration of more than 30%, preferred an upright position so it is more aligned to the phospholipid bilayer (Khelashvili and Harries, 2013). Therefore, in the bottom up process, the solvent concentration at the point of formation may impact of the orientation/alignment of cholesterol thus impacting on protein release. This manufacturing parameter controlled change in release profile, further demonstrating microfluidic is a versatile system. It can be fine-tuned to modify liposome attributes and the flow rate ratio is a key quality attribute which influences particle size, protein loading and protein release.

3.5 Continuous manufacture with at-line size analysis

High-throughput production of liposomes using microfluidics requires an ability to monitor liposome attributes during manufacturing. In particular, liposome size is a key product attribute given the impact this can have on drug loading, drug release and biodistribution. Therefore, the ability to monitor liposome size rapidly during production is a key element of a manufacturing process. To achieve this, we incorporated at-line (in real time) particle size monitoring using the Malvern Zetasizer AT (Malvern Instruments, Malvern, UK) both for in-process monitoring and for product validation (Figure 10). The sensitivity of this instrument was compared to the off-line characterising equipment (the Zetasizer Nano ZS) and two monitoring points in the production of DSPC:Chol liposomes were tested: in-process (directly after production) and the final purified product. The results in figure 10 confirm that the liposome size can be effectively monitored in real time (at-line) at both points in the process. After production, the liposome sizes recorded were 49 ± 0.4 nm when measured at-line compared with 50 ± 0.3 when measured off-line. Similarly, after purification, the final liposome product particle size was 52 ± 0.4 nm when measured at-line compared with 52 ± 0.7 nm when measured off-line. There was also no significant difference in the PDI measured by both instruments after microfluidics (~0.06 PDI) and post purification (~0.15 PDI), thus indicating a rapid at-line particle size analysis can be incorporated within this continuous and scalable-independent process for monitoring liposomal formulation quality in real-time.

4. Conclusions

We have successfully shown for the first time, a simple and scale-independent method to manufacture, purify and monitor the production of liposomes encapsulating proteins. This process gives high protein loading and can be undertaken at room temperature thereby circumventing any potential risk to the protein structure. Key process parameters identified are the lipid concentration, the liposome composition, the protein concentration and the flow rate ratio. This microfluidic manufacturing process ensures a quick and efficient process for the translation of novel liposome

formulations from the bench to production and de-risks the adoption of liposomes for wide-scale applications.

5. Acknowledgements

This work was part funded by the EPSRC Centre for Innovative Manufacturing in Emergent Therapies (EPSRC) and the University of Strathclyde. We would like to thank Malvern Panalytical for the use of the Zetasizer AT. JtH and MLB thank the EPSRC Centre for Innovative Manufacturing in Continuous Manufacturing and Crystallisation (http://www.cmac.ac.uk) for support (EPSRC funding under grant reference: EP/I033459/1).

6. Supporting information Available

Data presented in this publication can be found at [DOI to be confirmed on acceptance of manuscript].

References

Bulbake, U., Doppalapudi, S., Kommineni, N., Khan, W., 2017. Liposomal Formulations in Clinical Use: An Updated Review. Pharmaceutics 9, 12.

Carter, P.J., 2011. Introduction to current and future protein therapeutics: A protein engineering perspective. Experimental Cell Research 317, 1261-1269.

Carugo, D., Bottaro, E., Owen, J., Stride, E., Nastruzzi, C., 2016. Liposome production by microfluidics: potential and limiting factors. Scientific reports 6.

Chan, Y.-H., Chen, B.-H., Chiu, C.P., Lu, Y.-F., 2004. The influence of phytosterols on the encapsulation efficiency of cholesterol liposomes. International Journal of Food Science & Technology 39, 985-995.

Colletier, J.-P., Chaize, B., Winterhalter, M., Fournier, D., 2002. Protein encapsulation in liposomes: efficiency depends on interactions between protein and phospholipid bilayer. BMC biotechnology 2, 9.

Devaraj, G.N., Parakh, S., Devraj, R., Apte, S., Rao, B.R., Rambhau, D., 2002. Release studies on niosomes containing fatty alcohols as bilayer stabilizers instead of cholesterol. Journal of colloid and interface science 251, 360-365.

Dimov, N., Kastner, E., Hussain, M., Perrie, Y., Szita, N., 2017. Formation and purification of tailored liposomes for drug delivery using a module-based micro continuous-flow system. Scientific reports 7, 12045.

Epand, R.M., Epand, R.F., Maekawa, S., 2003. The arrangement of cholesterol in membranes and binding of NAP-22. Chemistry and physics of lipids 122, 33-39.

Fatouros, D.G., Antimisiaris, S.G., 2002. Effect of amphiphilic drugs on the stability and zeta-potential of their liposome formulations: a study with prednisolone, diazepam, and griseofulvin. Journal of colloid and interface science 251, 271-277.

Fosgerau, K., Hoffmann, T., 2015. Peptide therapeutics: current status and future directions. Drug Discovery Today 20, 122-128.

Gregoriadis, G., Davis, C., 1979. Stability of liposomes invivo and invitro is promoted by their cholesterol content and the presence of blood cells. Biochemical and Biophysical Research Communications 89, 1287-1293.

Gregoriadis, G., Leathwood, P., Ryman, B.E., 1971. Enzyme entrapment in liposomes. FEBS letters 14, 95-99.

Habjanec, L., Frkanec, R., Halassy, B., Tomašić, J., 2006. Effect of liposomal formulations and immunostimulating peptidoglycan monomer (PGM) on the immune reaction to ovalbumin in mice. Journal of liposome research 16, 1-16.

Huang, Y.-Y., Wang, C.-H., 2006. Pulmonary delivery of insulin by liposomal carriers. Journal of Controlled Release 113, 9-14.

ICH, I., Q3C (R6) Impurities: Guideline for Residual Solvents. 2016. There is no corresponding record for this reference.

Jahn, A., Stavis, S.M., Hong, J.S., Vreeland, W.N., DeVoe, D.L., Gaitan, M., 2010. Microfluidic Mixing and the Formation of Nanoscale Lipid Vesicles. ACS Nano 4, 2077-2087.

Jahn, A., Vreeland, W.N., DeVoe, D.L., Locascio, L.E., Gaitan, M., 2007. Microfluidic Directed Formation of Liposomes of Controlled Size. Langmuir 23, 6289-6293.

Joshi, S., Hussain, M.T., Roces, C.B., Anderluzzi, G., Kastner, E., Salmaso, S., Kirby, D.J., Perrie, Y., 2016. Microfluidics based manufacture of liposomes simultaneously entrapping hydrophilic and lipophilic drugs. International journal of pharmaceutics 514, 160-168.

Kastner, E., Kaur, R., Lowry, D., Moghaddam, B., Wilkinson, A., Perrie, Y., 2014. High-throughput manufacturing of size-tuned liposomes by a new microfluidics method using enhanced statistical tools for characterization. International Journal of Pharmaceutics 477, 361-368.

Kastner, E., Verma, V., Lowry, D., Perrie, Y., 2015. Microfluidic-controlled manufacture of liposomes for the solubilisation of a poorly water soluble drug. International journal of pharmaceutics 485, 122-130.

628 Khelashvili, G., Harries, D., 2013. How sterol tilt regulates properties and organization of lipid
629 membranes and membrane insertions. Chemistry and Physics of Lipids 169, 113-123.
630 Khelashvili, G., Pabst, G., Harries, D., 2010. Cholesterol orientation and tilt modulus in DMPC bilayers.
631 The Journal of Physical Chemistry B 114, 7524-7534.
632 Lapinski, M.M., Castro-Forero, A., Greiner, A.J., Ofoli, R.Y., Blanchard, G.J., 2007. Comparison of
633 liposomes formed by sonication and extrusion: rotational and translational diffusion of an embedded
634 chromophore. Langmuir 23, 11677-11683.
635 Lee, K.Y., Yuk, S.H., 2007. Polymeric protein delivery systems. Progress in Polymer Science 32, 669-
636 697.
637 Li, N., Peng, L.-H., Chen, X., Nakagawa, S., Gao, J.-Q., 2011. Effective transcutaneous immunization by
638 antigen-loaded flexible liposome in vivo. International Journal of Nanomedicine 6, 3241-3250.
639 Liu, W., Ye, A., Liu, W., Liu, C., Han, J., Singh, H., 2015. Behaviour of liposomes loaded with bovine
640 serum albumin during in vitro digestion. Food Chemistry 175, 16-24.
641 Lu, Y., Sun, W., Gu, Z., 2014. Stimuli-Responsive Nanomaterials for Therapeutic Protein Delivery.
642 Journal of controlled release : official journal of the Controlled Release Society 194, 1-19.
643 Mendez, R., Banerjee, S., 2017. Sonication-based basic protocol for liposome synthesis. Lipidomics:
644 Methods and Protocols, 255-260.
645 Moghaddam, B., Ali, M.H., Wilkhu, J., Kirby, D.J., Mohammed, A.R., Zheng, Q., Perrie, Y., 2011. The
646 application of monolayer studies in the understanding of liposomal formulations. International Journal
647 of Pharmaceutics 417, 235-244.
648 Mohammed, A., Weston, N., Coombes, A., Fitzgerald, M., Perrie, Y., 2004. Liposome formulation of
649 poorly water soluble drugs: optimisation of drug loading and ESEM analysis of stability. International
650 journal of pharmaceutics 285, 23-34.
651 Monteiro, N., Martins, A., Reis, R.L., Neves, N.M., 2014. Liposomes in tissue engineering and
652 regenerative medicine. Journal of the Royal Society Interface 11, 20140459.
653 Murao, A., Nishikawa, M., Managit, C., Wong, J., Kawakami, S., Yamashita, F., Hashida, M., 2002.
654 Targeting efficiency of galactosylated liposomes to hepatocytes in vivo: effect of lipid composition.
655 Pharmaceutical research 19, 1808-1814.
656 Oellers, M., Bunge, F., Vinayaka, P., Driesche, S.v.d., Vellekoop, M.J., 2017. Flow-Ratio Monitoring in a
657 Microchannel by Liquid-Liquid Interface Interferometry, Multidisciplinary Digital Publishing Institute
658 Proceedings, p. 498.
659 Panagi, Z., Avgoustakis, K., Evangelatos, G., Ithakissios, D., 1998. Protein-induced CF release from
660 liposomes in vitro and its correlation with the BLOOD/RES biodistribution of liposomes. International
661 journal of pharmaceutics 163, 103-114.
662 Paolinelli, C., Barteri, M., Boffi, F., Forastieri, F., Gaudiano, M.C., Della Longa, S., Castellano, A.C., 1997.
663 Structural differences of ovalbumin and S-ovalbumin revealed by denaturing conditions. Zeitschrift für
664 Naturforschung C 52, 645-653.
665 Patty, P.J., Frisken, B.J., 2003. The pressure-dependence of the size of extruded vesicles. Biophysical
666 journal 85, 996-1004.
667 Philippot, J.R., Schuber, F., 2017. Liposomes as Tools in Basic Research and Industry (1994). CRC press.
668 Ramaldes, G.A., Deverre, J.R., Grognet, J.M., Puisieux, F., Fattal, E., 1996. Use of an enzyme
669 immunoassay for the evaluation of entrapment efficiency and in vitro stability in intestinal fluids of
670 liposomal bovine serum albumin. International Journal of Pharmaceutics 143, 1-11.
671 Semple, S.C., Chonn, A., Cullis, P.R., 1996. Influence of cholesterol on the association of plasma
672 proteins with liposomes. Biochemistry 35, 2521-2525.
673 Stein, P.E., Leslie, A.G., Finch, J.T., Turnell, W.G., McLaughlin, P.J., Carrell, R.W., 1990. Crystal structure
674 of ovalbumin as a model for the reactive centre of serpins. Nature 347, 99.
675 Szoka, F., Papahadjopoulos, D., 1978. Procedure for preparation of liposomes with large internal
676 aqueous space and high capture by reverse-phase evaporation. Proceedings of the national academy
677 of sciences 75, 4194-4198.

678 Szoka Jr, F., Papahadjopoulos, D., 1980. Comparative properties and methods of preparation of lipid
679 vesicles (liposomes). Annual review of biophysics and bioengineering 9, 467-508.
680 Torchilin, V.P., Lukyanov, A.N., 2003. Peptide and protein drug delivery to and into tumors: challenges
681 and solutions. Drug Discovery Today 8, 259-266.
682 Usmani, S.S., Bedi, G., Samuel, J.S., Singh, S., Kalra, S., Kumar, P., Ahuja, A.A., Sharma, M., Gautam, A.,
683 Raghava, G.P.S., 2017. THPdb: Database of FDA-approved peptide and protein therapeutics. PLOS ONE
684 12, e0181748.
685 Vila-Caballer, M., Codolo, G., Munari, F., Malfanti, A., Fassan, M., Rugge, M., Balasso, A., de Bernard,
686 M., Salmaso, S., 2016. A pH-sensitive stearoyl-PEG-poly(methacryloyl sulfadimethoxine)-decorated
687 liposome system for protein delivery: An application for bladder cancer treatment. Journal of
688 Controlled Release 238, 31-42.
689 Xu, X., Costa, A., Burgess, D.J., 2012. Protein encapsulation in unilamellar liposomes: high
690 encapsulation efficiency and a novel technique to assess lipid-protein interaction. Pharmaceutical
691 research 29, 1919-1931.
692 Zizzari, A., Bianco, M., Carbone, L., Perrone, E., Amato, F., Maruccio, G., Rendina, F., Arima, V., 2017.
693 Continuous-Flow Production of Injectable Liposomes via a Microfluidic Approach. Materials 10, 1411.

694

Tables

Table 1. Examples of traditional methods used to entrap proteins within liposomes and their relative entrapment efficiencies. The efficiency of neutral and anionic liposomes to encapsulate protein was investigated relative to the manufacturing methods.

Protein loaded	Liposome formulation	Production technique	Protein loading	Reference
Bovine serum albumin	soyabean PC/DSPC, cholesterol, phosphatidylglycerol	Thin film lipid hydration.	0.1 mg/mL	(Ramaldes et al., 1996)
Bovine serum albumin	PC:Chol	Dehydration-rehydration method.	28%	(Chan et al., 2004)
Bovine Serum Albumin	PC:Chol:Tween:Vitamin E	Thin film lipid hydration.	34 ± 9%	(Liu et al., 2015)
Bovine Serum Albumin	Soybean PC:Chol	Thin film lipid hydration.	22-32%.	(Vila-Caballer et al., 2016)
Ovalbumin	PC:Chol	Thin film lipid hydration.	10%	(Habjanec et al., 2006)
Ovalbumin	Phospholipid S, Chol (very high lipid concentration, 200 mg)	Thin film lipid hydration.	48% ± 9%	(Li et al., 2011)
Amyloglucosidase, Albumin	PC:Chol:Dicetylphosphate	Lipid film hydration	4 - 6.5%, 6.8 - 10.6%	(Gregoriadis et al., 1971)
Superoxide dismutase	DPPC:Chol DSPC:Chol	Unilamellar vesicles mixed with freeze-thaw cycling	50%	(Xu et al., 2012)
Acetylcholinesterase	Egg PC	Thin film lipid hydration.	35%	(Colletier et al., 2002)
Insulin	Hydrogenated PC:Chol	Thin film lipid hydration.	28% (4°C) 30% (25°C) and 50% (40°C)	(Huang and Wang, 2006)

Table 2. Lipid recovery in liposomes produced by microfluidics. Four liposomal formulations (PC:Chol, DMPC:Chol, DPPC:Chol and DSPC:Chol each at 2:1 wt/wt) were manufactured using microfluidics at a flow rate ratio of 3:1, 15 mL/min TFR and purified using dialysis. Lipid recovery was calculated using HPLC-ELSD. Results represent mean ± SD, n=3 independent batches.

	Lipid recovery (% of initial amount)							
Formulation	PC:Chol		DMPC:Chol		DPPC:Chol		DSPC:Chol	
Lipid	PC	Chol	DMPC	Chol	DPPC	Chol	DSPC	Chol
Recovery	94 ± 5.0	95 ± 2.3	95 ± 1.6	96 ± 1.0	96 ± 1.2	97 ± 2.7	98 ± 5.7	97 ± 3.8

Table 3. Comparison of particle size of liposomes formulated from phospholipids of different phase transition temperatures manufactured via microfluidics. Two liposome formulations (DSPC:Chol (10:5 wt/wt) and DOPC:Chol (10:5 wt/wt), initial lipid concentration of 1 mg/mL) were manufactured using microfluidics at a flow rate ratio of 3:1, 15 mL/min TFR and purified using dialysis. Results represent mean ± SD, n=3 independent batches.

	Carbon chain length	Tm (°C)	Saturation	Particle size (nm)	PDI
DOPC	18 carbons	-17	18:1c9	84.9 ± 4.3	0.13 ± 0.04
DSPC	18 carbons	55	18:0	41.5 ± 0.2	0.03 ± 0.01

Table 4. Comparison of entrapment of different proteins. In total three different proteins (Insulin, Bovine Serum Albumin (BSA) and OVA) were incorporated into DSPC:Chol liposomes (2:1 wt/wt) manufactured using microfluidics at a flow rate ratio of 3:1, 15 mL/min TFR and purified via TFF. An initial protein concentration of 250 µg/mL was employed. Results represent mean ± SD, n=3 independent batches.

Protein	**Protein Loading (% of initial amount added)**	**Liposome Size (d.nm)**	**Liposome PDI**
Insulin (5.7 KDa)	36.8 ± 2.7	57 ± 2.9	0.087 ± 0.062
OVA (42.7 KDa)	34.2 ± 4.9	53 ± 2.5	0.219 ±0.011
BSA (65.5 KDa)	25.2 ± 2.8	65 ± 2.8	0.144 ± 0.021

Figures.

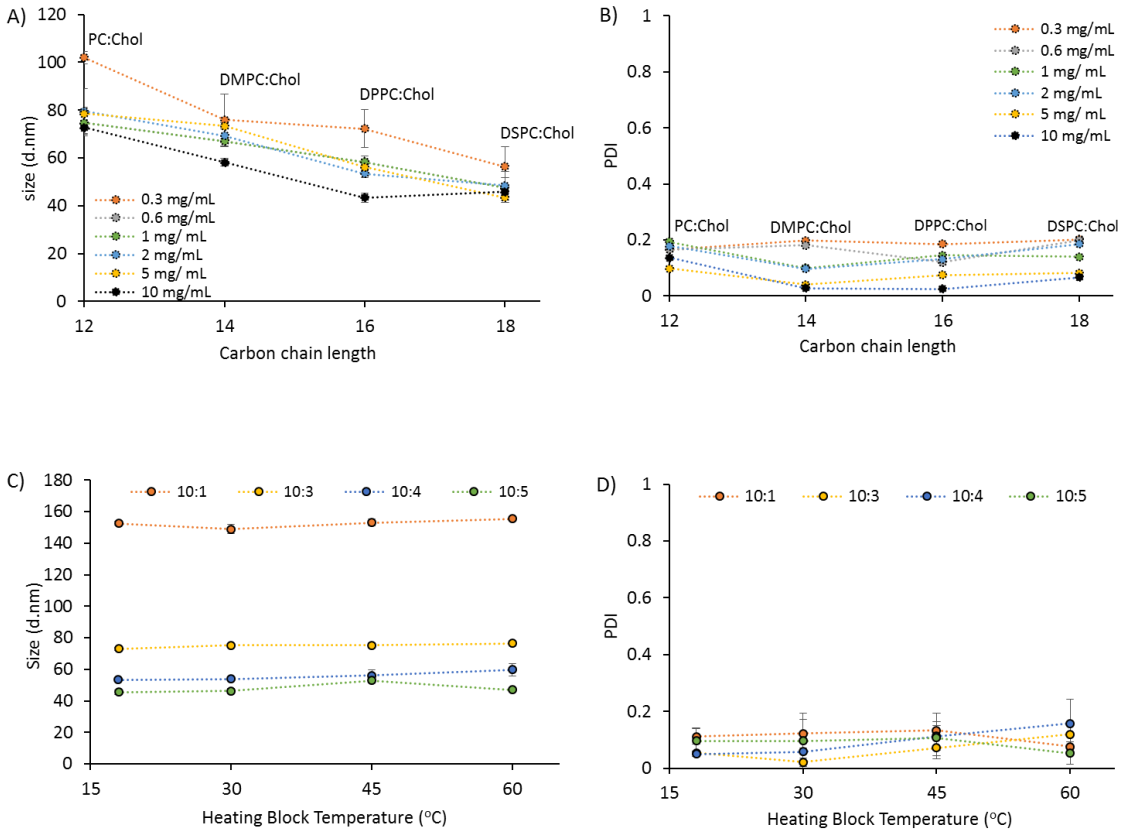

Figure 1: The effect of liposomal formulation on physicochemical characteristics of liposomes produced by micofluidics. Four liposome formulations (PC:Chol, DMPC:Chol, DPPC:Chol, and DSPC:Chol) with increasing hydrocarbon tail length were manufactured using microfluidics at a 3:1 FRR, 15 mL/min TFR and purified using dialysis. The effect of PC lipid chain length on A) liposomes z-average size (d.nm) and B) PDI. DSPC:Chol liposomes were selected and the effect of cholesterol content and heating block temperature were investigated in regards to C) z-average particle size and D) PDI. Results represent mean ± SD, n=3 independent batches.

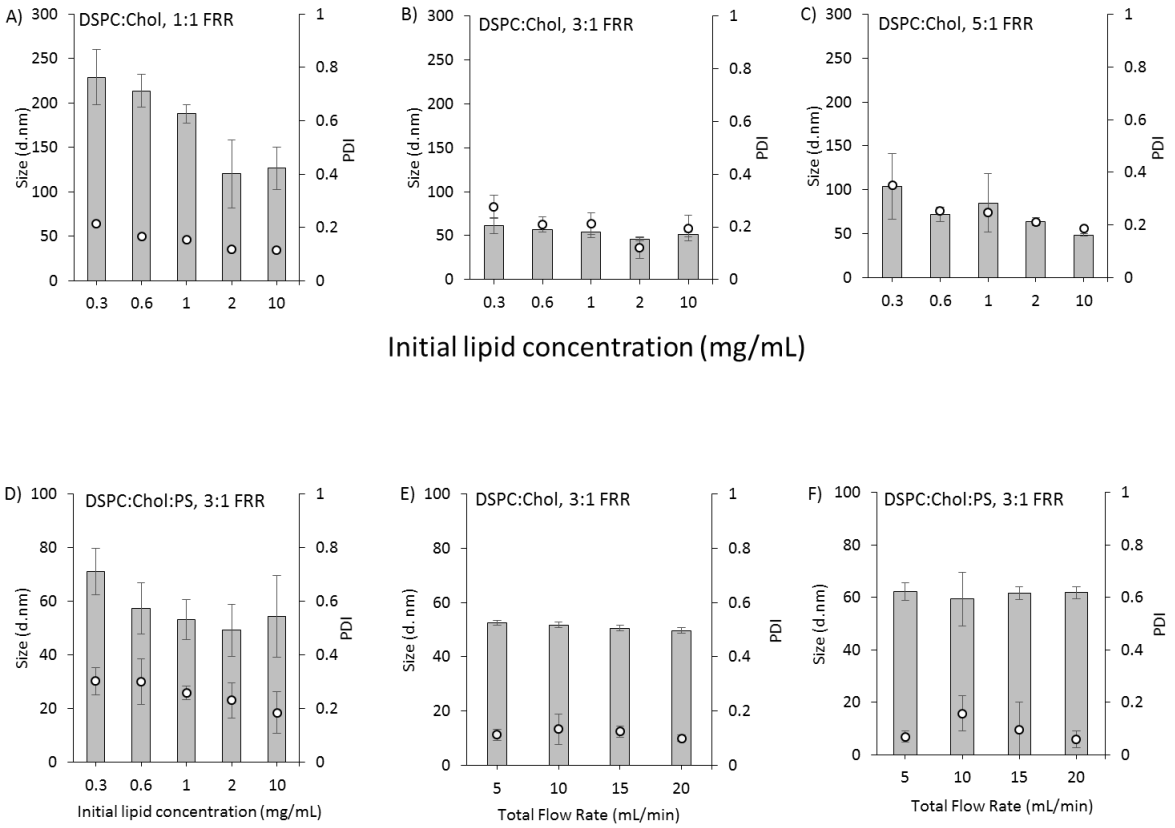

Figure 2: The effect of microfluidic parameters on neutral and anionic liposome attributes. The effect of the initial lipid concentration on average liposome size (d.nm; represented by bars) and PDI (represented by discrete points) for liposomal formulation DSPC:Chol (10:5 wt/wt) (10 mL/min TFR) at a flow rate ratio of A) 1:1, B) 3:1, and C) 5:1. D) The effect of increasing initial lipid concentration on z-average particle size (d.nm) for DSPC:Chol:PS (10:5:4 wt/wt) (3:1 FRR, 10 mL/min TFR). E) Investigating the effect total flow rate (mL/min) on z-average particle size (d.nm) and PDI for liposomal formulation DSPC:Chol (4 mg/mL initial lipid, 3:1 FRR). F) The effect of total flow rate (mL/min) for anionic formulation DSPC:Chol:PS (4 mg/mL initial lipid, 3:1 FRR). Results represent mean ± SD, n =3 of independent batches.

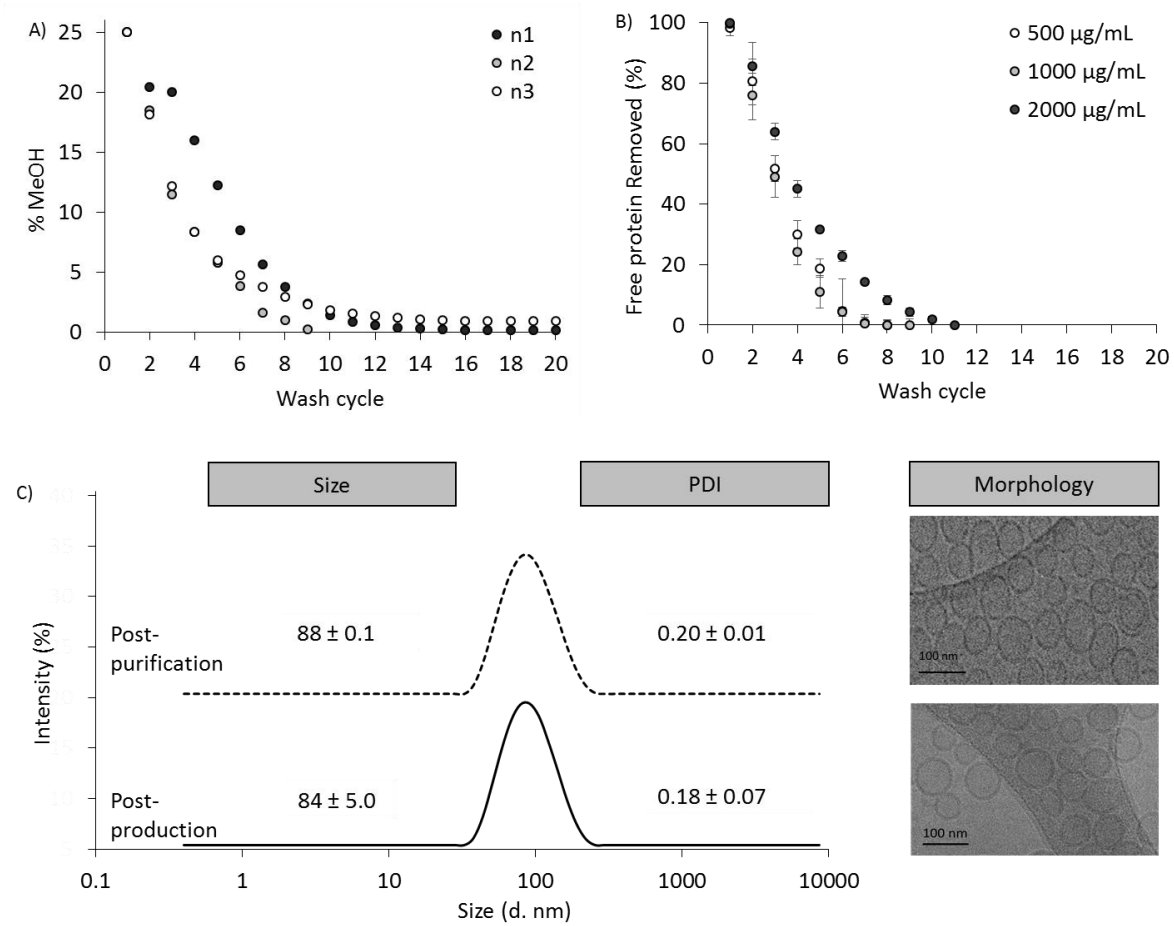

738
739 Figure 3: Purification of liposomes using tangential flow filtration (TFF). Liposomes (DPPC:Chol; FRR
740 3:1, 15 mL/min TFR) were prepared and characterised as follows: A) Residual solvent (methanol)
741 remaining in liposomes after consecutive wash cycles, B) removal of non-incorporated protein via TFF,
742 C) liposome attributes before and after purification via TFF and cryo-EM images of liposomes before
743 and after TFF purification. Results represent mean ± SD, n =3 of independent batches.

744

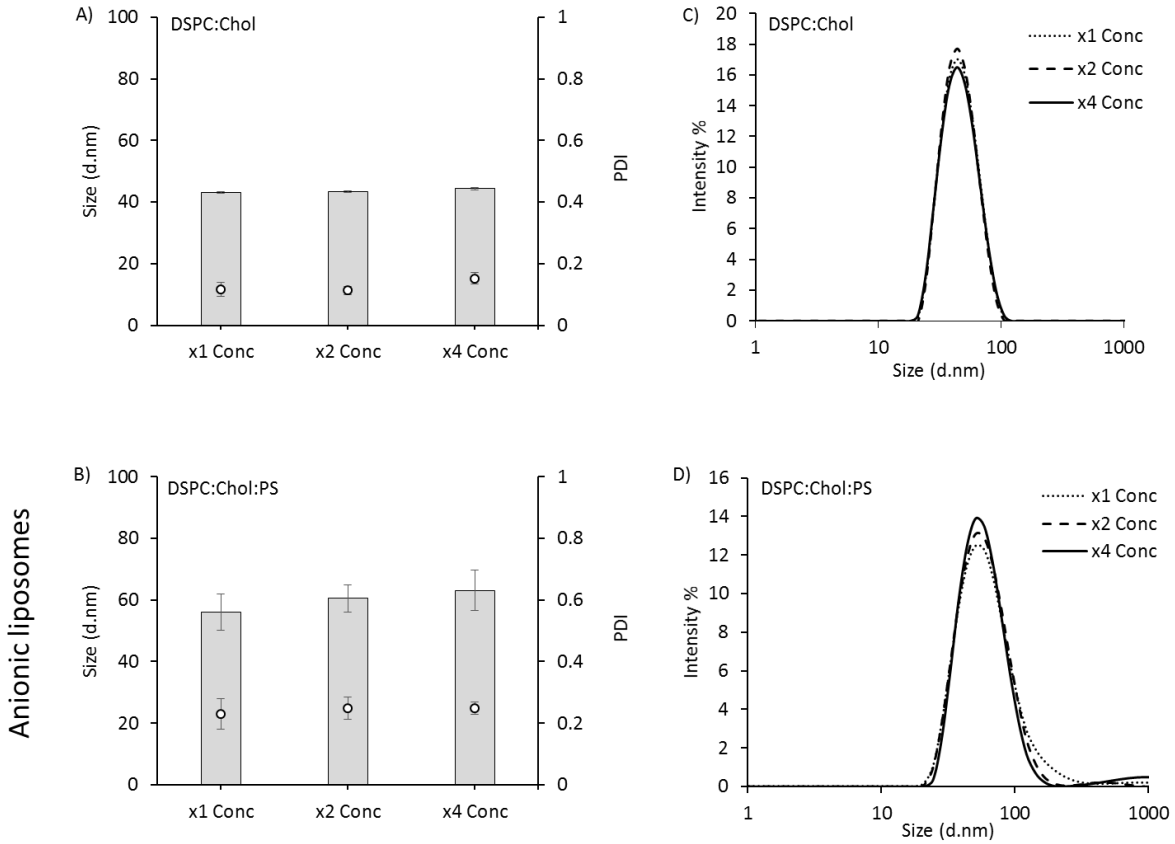

Figure 4: Concentration of liposomal formulations using tangential flow filtration. DSPC:Chol (10:5 wt/wt) and DSPC:Chol:PS (10:5:4 wt/wt) were prepared at 4 mg/mL initial lipid concentration, 3:1 FRR, 15 mL/min TFR following microfluidics, followed by 1,2 and 4 fold concentration steps. Particle Size (Z-Avg; represented by bars) and PDI (represented by discrete points) for A) DSPC:Chol and B) DSPC:Chol:PS both prepared C) and D) are intensity plots for the same conditions. Results represent mean ± SD, n =3 of independent batches.

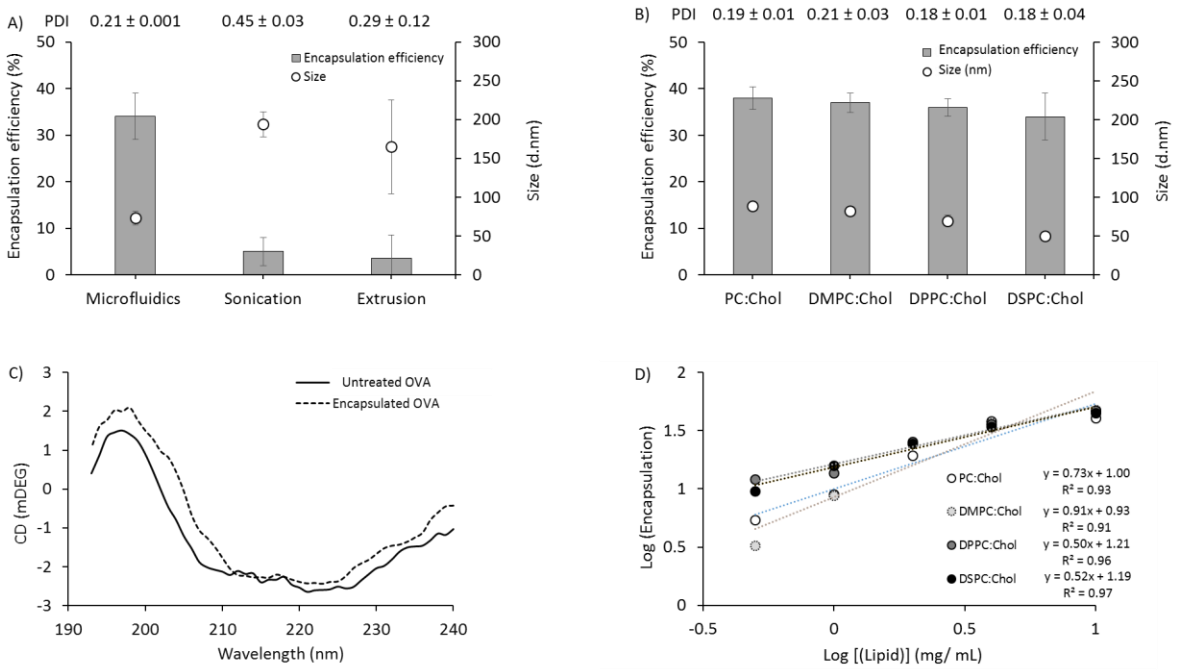

Figure 5. Manufacture of protein loaded liposomes using microfluidics. A) Ovalbumin loading and physicochemical comparison between microfluidics and lipid-film hydration followed by extrusion or sonication. DSPC:Chol (10:5 wt/wt) liposomes were made with 1 mg/mL final total lipid and 0.18 mg/mL ovalbumin. The encapsulation efficiency, size and PDI of the liposomes. B) Microfluidics was further tested with respect to changes in lipid hydrocarbon tail length and concentration. Protein encapsulation, size and PDI for PC:Chol, DMPC:Chol, DPPC:Chol and DSPC:Chol (4 mg/ mL initial lipid and 0.25 mg/ mL Ovalbumin) made using microfluidics (3:1 FRR and 15 mL/ min TFR). C) The structural integrity of ovalbumin loaded into the liposomes measured by circular dichroism. DSPC:Chol (10:5 wt/wt) liposomes were prepared with OVA (8 mg/mL initial total lipid and OVA, 3:1 FRR, 15 mL/min TFR) and purified via TFF. Spectra was measured across 180 – 260 nm D) Log-log plot of lipid concentrations (0.5- 10 mg/ mL) against encapsulation efficiency (0.25 mg/ mL ovalbumin). Results represent mean ± SD, n=3 independent batches.

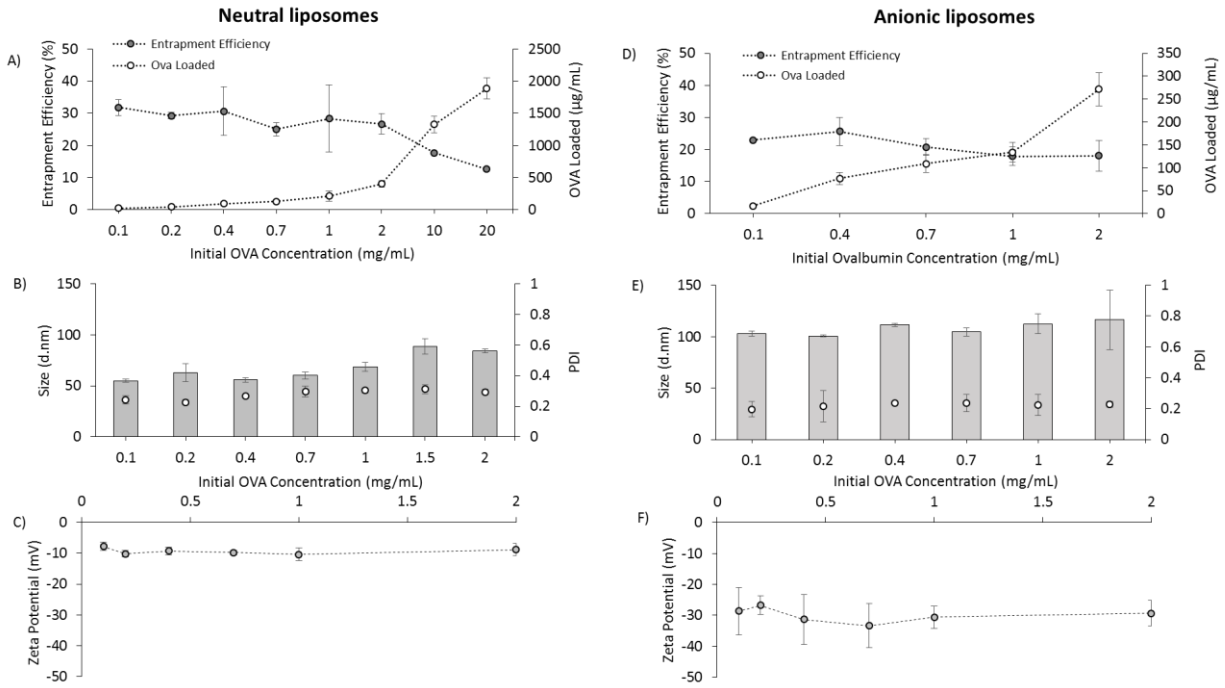

Figure 6: The effect of protein concentration in aqueous phase on entrapment efficiency and liposomal physicochemical characteristics for a neutral liposomal formulation (DSPC:Chol; 10:5 wt/wt) (A to C) and anionic formulation (DSPC:Chol:PS; 10:5:4 wt/wt) (D to F) using initial total lipid concentration of 4 mg/mL, 3:1 flow rate ratio and 15 mL/min TFR. A) Entrapment efficiency and protein loading across initial ovalbumin concentrations for neutral liposomal formulation. B) Average particle size and PDI, and C) Zeta potential for the same formulation. D) Entrapment efficiency and protein loading across initial ovalbumin concentrations for anionic liposomal formulation, E) Average particle size and PDI and, F) Zeta potential for the same formulation. In B) and E) particle size is shown by bars and PDI is shown by discrete points. Results represent mean ± SD, n=3 of independent batches.

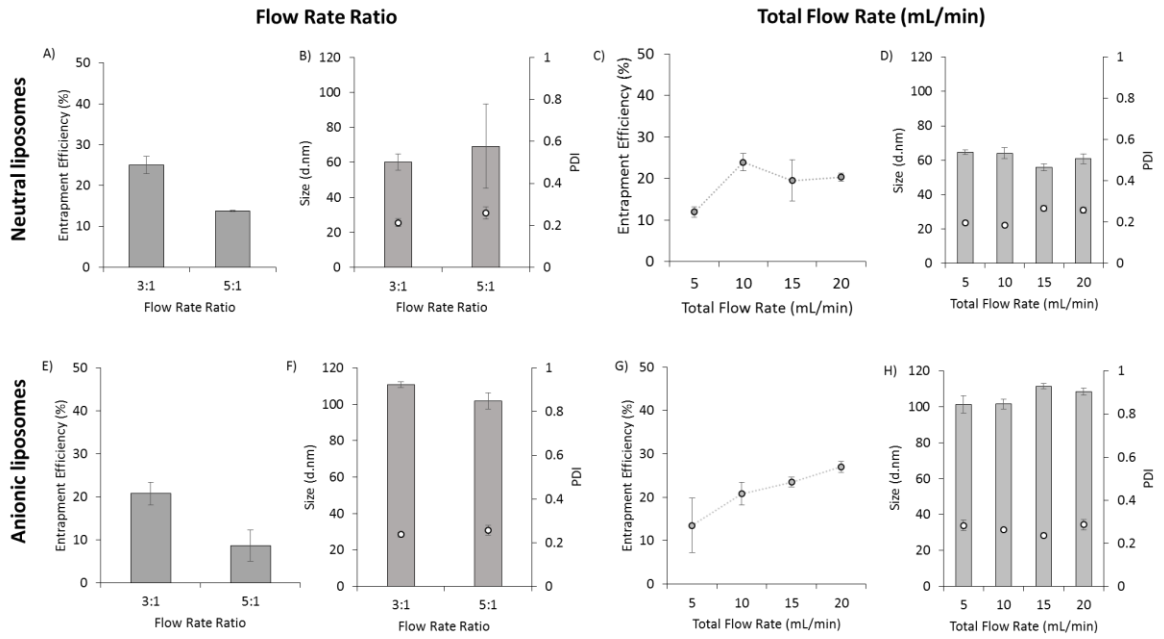

Figure 7: Microfluidic manufacture of neutral and anionic liposomes encapsulating protein. Both neutral (DSPC:Chol; 10:5 wt/wt) (A to D) and anionic (DSPC:Chol:PS; 10:5:4 wt/wt) (E to H) were tested: A) Entrapment efficiencies for flow rate ratios 3:1 and 5:1 for DSPC:Chol (final lipid and OVA concentrations matched at 1 mg/mL and 0.525 mg/mL respectively). B) Average particle size and PDI for the same formulation C) Entrapment efficiencies with varying on total flow rate (mL/min) (3:1 flow rate ratio, 4 mg/mL and 0.7 mg/mL initial total lipid and OVA respectively) and D) the resulting particle size (d.nm) and PDI with varying total flow rate. E) Effect of flow rate ratio on entrapment efficiency for DSPC:Chol:PS (final lipid and OVA concentrations matched at 1 mg/mL and 0.525 mg/mL respectively). F) Entrapment efficiencies with varying on total flow rate (mL/min) (3:1 flow rate ratio, 4 mg/mL and 0.7 mg/mL initial total lipid and OVA respectively) and H) the resulting particle size (d.nm) and PDI with varying total flow rate. Where appropriate liposome size is shown by bars and PDI is shown by discrete points. Results represent mean ± SD, n=3 of independent batches.

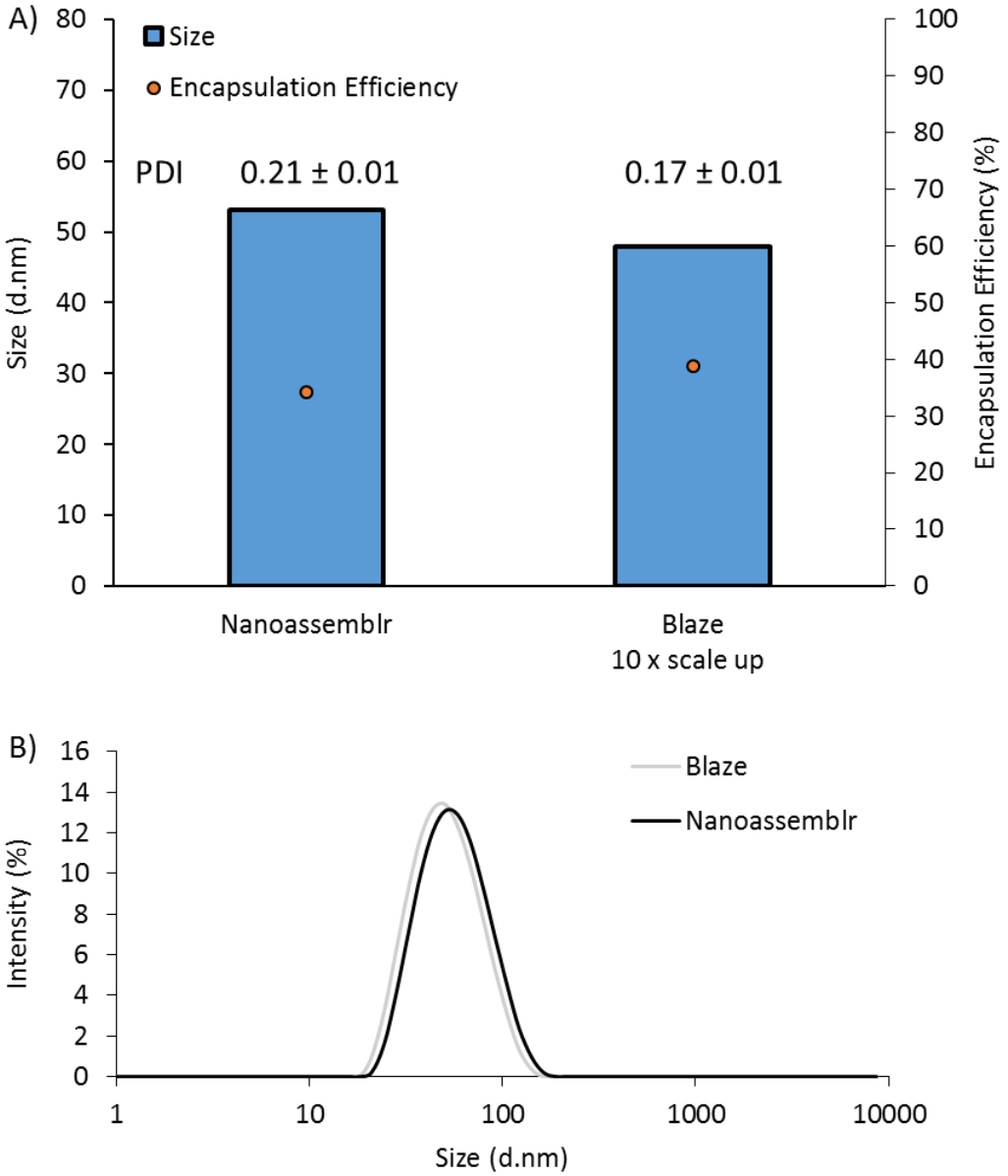

792
793 Figure 8: Proof-of-concept scale-out studies. DSPC:Chol liposomes were prepared at a FFR 3:1, TFR 15
794 mL/min, and a concentration of 10 mg/mL on both the NanoAssemblr (total volume 2 mL) and Blaze
795 (total volume 20 mL). A) The protein loading, size and polydispersity index (PDI) of both batches and
796 B) an overlay of the intensity plots for both batches.

797

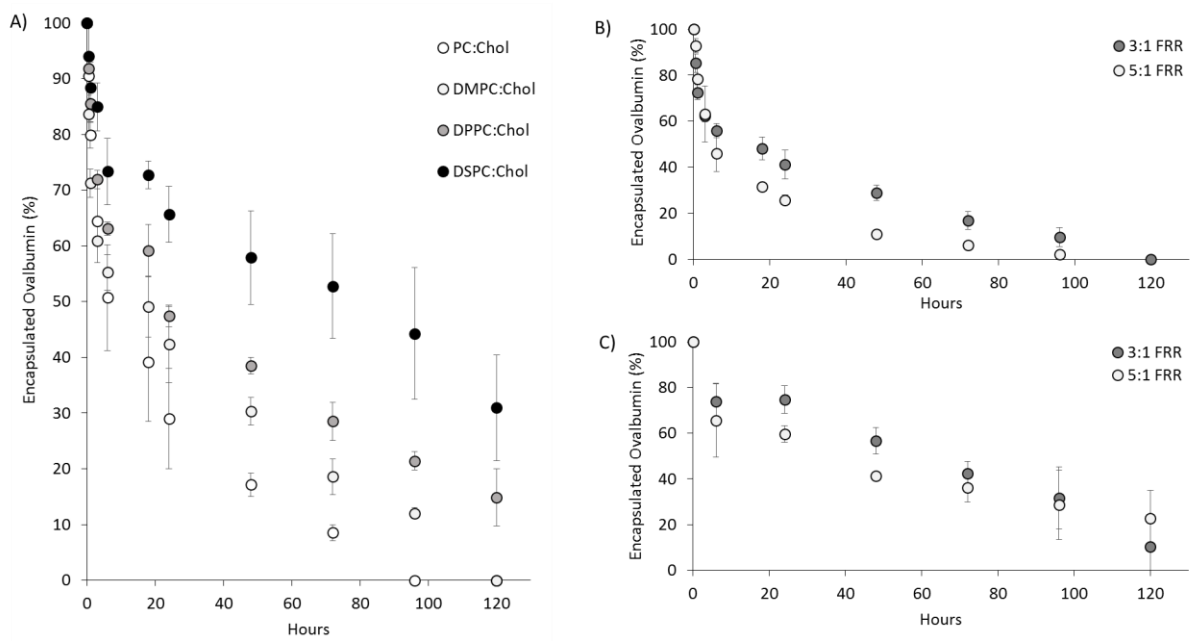

Figure 9. Protein release from liposome formulations manufactured by microfluidics. A) The release of OVA from PC:Chol, DMPC:Chol, DPPC:Chol and DSPC:Chol liposomes produced at a 3:1 ratio (15 mL/mi TFR) over 120 hours. B) Ovalbumin release from DMPC:Chol liposomes produced at a 3:1 and 5:1 FRR (15 mL/min TFR.) C) Ovalbumin release from DSPC:Chol liposomes produced at a 3:1 and 5:1 FRR (15 mL/min TFR, matched at a final concentration of 1 mg/mL total lipid, 0.1875 mg/mL OVA) Liposome suspensions were kept at 37°C with agitation. At set times, the sample was collected the OVA remaining inside the liposomes quantified. The results represent the mean of three independent batches ± SD.

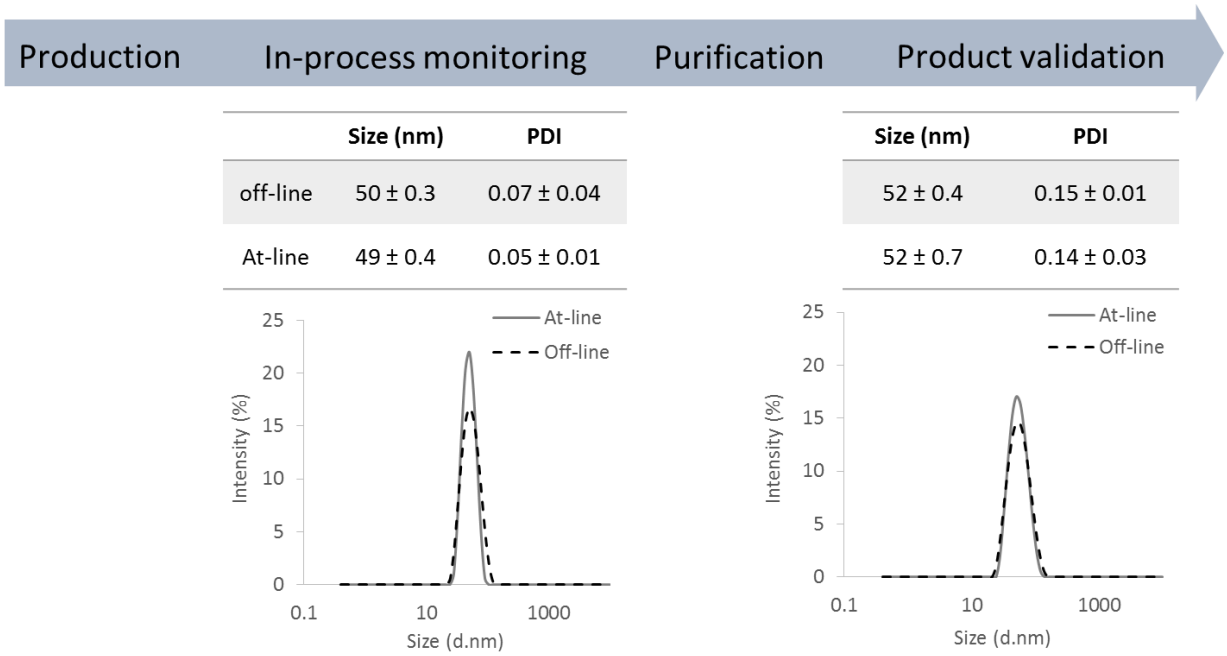

Figure 10: Liposome at-line particle size monitoring as part of a production train. DSPC:Chol liposomes were prepared at a FFR 3:1, TFR 15 mL/min, and a concentration of 10 mg/mL. The size and polydispersity index (PDI) of all formulations were measured (at a ratio of 1:10) off-line using the Zetasizer Nano ZS (Malvern Instruments, Malvern, UK) or at-line as part of the automated continuous manufacturing process using the Zetasizer AT (Malvern Instruments, Malvern, UK). To characterise liposomes in real time, the Zetasizer AT measured liposome size and PDI at a 1:10 dilution (liposomes to buffer), with adjustments to the automated mixing possible. The buffer (5 mL/min) and liposome formulation (0.5 mL/min) are taken up by the instrument, and enter into the flow cell where the size and PDI was measured. A total of 1 mL was required for each size measurement. Liposome formulations were purified using the KrosFlo Research Iii TFF system.